FERMILAB-Pub-92/217-A
UCLA/92/TEP/27
August, 1992

Large- and Small-Scale Constraints on Power Spectra in $\Omega = 1$ Universes

James M. Gelb[1], Ben-Ami Gradwohl[1,2], and Joshua A. Frieman[1]

[1]NASA/Fermilab Astrophysics Center
Fermi National Accelerator Laboratory
P.O. Box 500, Batavia, IL 60510

[2]Department of Physics
University of California Los Angeles
Los Angeles, CA 90024

ABSTRACT

The cold dark matter (CDM) model of structure formation, normalized on large scales, leads to excessive pairwise velocity dispersions on small scales. In an attempt to circumvent this problem, we study three scenarios (all with $\Omega = 1$) with more large-scale and less small-scale power than the CDM model: 1) an admixture of cold and hot dark matter; 2) cold dark matter with a non-scale-invariant power spectrum; and 3) cold dark matter with coupling of dark matter to a long-range vector field. Despite the reduced small-scale power, when such models are evolved to large amplitude, the velocities on small scales are actually *increased* over CDM with the same value of σ_8. This 'flip-over', in disagreement with the expectation from linear perturbation theory, arises from the nonlinear coupling of the extra power on large scales with shorter wavelengths. However, the recent COBE DMR results indicate smaller amplitudes for these models, $\sigma_8 \sim 0.5 - 0.7$, than for CDM (for which $\sigma_8 \sim 1.2$). Therefore, when normalized to COBE on large scales, such models do lead to reduced velocities on small scales and they produce fewer halos compared with CDM. Quantitatively it seems, however, that models that produce sufficiently low small-scale velocities fail to produce an adequate number of halos.

Subject headings: cosmology:dark matter—galaxies:formation

Submitted to Astrophysical Journal Letters

1. INTRODUCTION

Recent observations of fluctuations in the cosmic microwave background by the COBE satellite (Smoot et al. 1992) have placed the gravitational instability theory of structure formation on firmer footing. The shape of the linear density fluctuation spectrum is now constrained by a variety of observations ranging from galaxy scales ($\sim$ Mpc) up to the very large scales ($\sim$ 1000 Mpc) probed by COBE. The most popular theory of galaxy formation, the cold dark matter model with a scale-invariant spectrum of primordial fluctuations (hereafter CDM), has been studied by many authors using numerical N-body simulations over a wide range of scales (*e.g.* Davis et al. 1985, hereafter DEFW; Melott 1990; Park 1990; Couchman & Carlberg 1992; Gelb 1992, hereafter G92). It is difficult to reconcile the COBE DMR measurements, which indicate a rather high amplitude for CDM, with the observed low galaxy pairwise velocity dispersions on small scales. In a search for solutions to this problem, we consider three variant models with less small-scale and more large-scale power than CDM.

The amplitudes of the initial power spectra for the models are free parameters. It is common to normalize spectra by setting the *rms* density fluctuation in spheres of radii 16 Mpc to σ_8, assuming linear growth of modes independent of wavenumber k. (We assume $H_0 = 50\,\mathrm{km\,s^{-1}\,sec^{-1}}$ and $\Omega = 1$ throughout.) Thus, for a power spectrum $P(k)$,

$$\sigma_8^2 \equiv \int_0^\infty d^3k P(k) W_{\rm TH}^2(kR)\,;\ \ W_{\rm TH}(kR) = \frac{3}{(kR)^3}(\sin kR - kR\cos kR)\,;\ \ R = 16\,\mathrm{Mpc}\,. \quad (1)$$

On small scales, σ_8 is constrained by the pairwise velocity dispersion, $\sigma_{||}$, defined as the *rms* velocity along lines of separation of galaxy pairs: $\sigma_{||}(r) \equiv \langle (v_{||} - \langle v_{||}\rangle)^2\rangle^{1/2}$, where $v_{||} = (\vec{v}_2 - \vec{v}_1)\cdot\vec{r}/r$ is the parallel, peculiar velocity and $\vec{r} = \vec{r}_2 - \vec{r}_1$.

The pairwise velocity dispersion of galaxies on small scales was determined from redshift surveys by Davis & Peebles (1983): $\sigma_{||}$ ($r \lesssim 3$ Mpc) $\simeq 300 \pm 50\,\mathrm{km\,s^{-1}}$ (Bean et al. 1983 found $250 \pm 50\,\mathrm{km\,s^{-1}}$). Researchers have compared this value with N-body simulations in order to constrain the CDM model amplitude σ_8. DEFW found $\sigma_8 = 0.4$ and G92 found $\sigma_8 \lesssim 0.5$. However, the recent COBE measurements imply a larger amplitude for the CDM model: the observed *rms* fluctuation on 10°, $[\sigma_T(10°)]_{\rm DMR} =$

$(1.085 \pm 0.183) \times 10^{-5}$, sets $\sigma_8 \simeq 1.17 \pm 0.23$ [Adams et al. 1992; a nearly identical range for σ_8 is obtained by fitting the COBE angular correlation function $C(\theta)$]. A larger amplitude ($\sigma_8 \simeq 1.29[1^{+.38}_{-.65}]$, Adams et al. 1992) is also required for CDM by the large-scale peculiar velocities of galaxies, determined by Bertschinger et al. (1990) using the POTENT reconstruction algorithm. Thus, for CDM, large-scale observations suggest a σ_8 amplitude roughly *twice as large* as that indicated by $\sigma_{\|}$ on small scales.

A possible way to reconcile large scales with small scales was suggested by Couchman & Carlberg (1992), who found that $\sigma_{\|}$ for the resolved halos is a factor ~ 2 lower than $\sigma_{\|}$ for the mass, an effect known as 'velocity bias': $b_v \equiv \sigma_{\|}(\text{halos})/\sigma_{\|}(\text{mass})$. However, high amplitude CDM still produces $\sigma_{\|}$ in excess of the observed $\sigma_{\|}$. Furthermore, CDM simulations result in an overproduction of halos, with the high-mass halos (from mergers) possibly representing clusters. If so, then dividing up the clusters into halos eliminates the velocity bias altogether (see G92). The alternative approach of using peak particles to represent galaxies also leads to $b_v \simeq 1$ (DEFW; Katz, Quinn, & Gelb 1992). We therefore claim, that $\sigma_{\|}(\text{mass})$ adequately reflects $\sigma_{\|}(\text{halos})$, and consequently only focus on $\sigma_{\|}(\text{mass})$ in the following analysis.

2. MODELS

We present results from 128^3 particle simulations using the particle-mesh technique on a 256^3 grid (Bertschinger & Gelb 1991) in boxes of comoving length 200 Mpc on a side. This size is large enough to encompass the waves that contribute significantly to σ_8 and $\sigma_{\|}$, although these simulations, with particle mass $2.6 \times 10^{11} M_\odot$, are inadequate for resolving individual halos. (We use smaller boxes at the end of §4 to study halo formation.)

We explore three models with less small-scale and more large-scale power than the CDM model: (1) models with an admixture of hot and cold dark matter (using the density-weighted power spectrum of van Dalen & Schaefer 1991 with cold particles); (2) a cold dark matter model with a non-scale-invariant, power-law primordial spectrum, $P(k) \propto k^n$, with $n = 0.7$ and a DEFW transfer function; and (3) cold dark matter models in which the dark matter couples to a hypothetical long-range field (Frieman & Gradwohl 1991; Gradwohl & Frieman 1992). In all cases, we assume negligible baryon

density, and, with the exception of (2), a scale-invariant ($n = 1$) primordial spectrum.

In case (3), the 'alpha' models, the force law between objects of mass m is:

$$r^2 F/(Gm^2) = 1 + \alpha(1 + r/\lambda_0)\exp(-r/\lambda_0) \ , \qquad (2)$$

so that gravity is effectively retarded for $\alpha < 0$, *i.e.* in the case of a vector field. Here, α is a measure of the relative strength of the new force, and λ_0 is its physical range. At each timestep, we regenerate the optimal Green's function of the potential associated with the force law of eqn. 2.

Other authors have studied some of these models. Cen et al. (1992) simulated a $\sigma_8 = 0.5$ $n = 0.7$ cold dark matter model with comparable resolution. The authors argued that this model has lower $\sigma_{\parallel} \sim 400 - 500\,\mathrm{km\,s^{-1}}$ than $\sigma_8 = 1$ CDM, but that a velocity bias $b_v \simeq 1/1.5$ is still needed to match the observed $\sigma_{\parallel} \sim 300\,\mathrm{km\,s^{-1}}$. However, we do not allow a velocity bias factor for reasons discussed earlier. Davis, Summers, & Schlegel (1992) performed high resolution simulations with separate cold and hot dark matter particles ($\Omega_{\rm HDM} = 0.30$) in 14 Mpc boxes at $\sigma_8 = 0.9$. We demonstrate that this box is too small to adequately measure $\sigma_{\parallel}$ (as pointed out by the authors).

3. LINEAR PERTURBATIONS

The dimensionless linear power spectra are shown in fig. 1a for $L = 200$ Mpc. We begin all simulations at an expansion factor $a = 1/50$ with $a = 1$ when $\sigma_8 = 1$. Results are shown for CDM (standard cold dark matter); C+H13 and C+H30 (cold dark matter mixed with 13% and 30% hot dark matter); TILT7 (cold dark matter with $n = 0.7$); and ALPHA3 and ALPHA5 (cold dark matter models with $\alpha = -0.3$, $\lambda_0 = 100$ kpc; and $\alpha = -0.5$, $\lambda_0 = 500$ kpc).

The TILT7, C+H13, and ALPHA3 power spectra are similar, yet the alpha simulations lag behind as the modified force law continues to retard the subsequent evolution. Note that our simplified cold plus hot models neglect the continual damping effect associated with the free-streaming of the hot component and is therefore likely to overestimate $\sigma_{\parallel}$.

It is instructive to estimate $\sigma_{\parallel}$ in linear perturbation theory. From $\vec{\nabla}\cdot\vec{v} \approx -H_0\Omega^{4/7}\delta$ (Peebles 1980; Lightman & Schechter 1990), where δ is the density contrast, we find

$v_k^2 d^3k \propto H_0^2 P(k)/k^2 d^3k$, and hence the linear estimate

$$\sigma_{\parallel}^2(r) \equiv \langle |\vec{v}(r) - \vec{v}(0)|^2 \rangle = 2[\langle v^2 \rangle - \langle \vec{v}(r) \cdot \vec{v}(0) \rangle]$$

$$= 2H_0^2 \int_{2\pi/L}^{\infty} 4\pi k^2 dk \frac{P(k)}{k^2} \left[1 - \frac{\sin kr}{kr}\right] . \quad (3)$$

The factor $1 - \sin(kr)/(kr)$ filters out the contribution of long waves to the small-scale pairwise velocity dispersion. This is opposite to the top hat filter $W_{\rm TH}$ in eqn. 1.

In fig. 2a we plot linear theory estimates of $\sigma_{\parallel}$ for the various spectra at $\sigma_8 = 1$. The models with reduced small-scale power appear to fare well with the observations at these scales, but, as we now show, nonlinear effects radically alter $\sigma_{\parallel}$.

4. NONLINEAR CALCULATIONS

4.1 PAIRWISE VELOCITY DISPERSIONS

In fig. 1b we present nonlinear power spectra at $\sigma_8 = 1$. For low values of k, the spectra agree with their counterparts in fig. 1a, indicating a sufficiently large box size. The models with less small-scale power in the initial conditions continue to have less small-scale power in the nonlinear regime, yet the nonlinear spectral shapes and the differences among the models are significantly altered.

The nonlinear $\sigma_{\parallel}$ for the models are shown in figs. 2b and 2c. Comparing with fig. 2a, it is clear that linear theory is a very poor estimator of both the amplitude and the general characteristics of $\sigma_{\parallel}$. In fig. 2b $\sigma_{\parallel}$ is shown at various σ_8 for CDM and C+H30. At low amplitude, $\sigma_8 \lesssim 0.5$, $\sigma_{\parallel}$ for C+H30 is lower than $\sigma_{\parallel}$ for CDM, in agreement with the expectation from linear theory. However, when the models are evolved further, $\sigma_{\parallel}$ 'flips over': despite its reduced small-scale power, the C+H30 model yields *larger* $\sigma_{\parallel}$ than CDM. Fig. 2c shows that this flip-over at high σ_8 (even for the continually damped alpha model) is generic for these models; it is a reflection of the fact that extra power on large scales couples significantly to small scales. This effect is manifest in the pairwise velocity dispersion, but not the power spectrum, because the former is more sensitive to long wavelengths. The flip-over in the initial power spectra occurs on scales exceeding ~ 75 Mpc (fig. 1a) and is therefore missed in small boxes. Originally we used 51.2 Mpc boxes and did not see this effect.

We now fix the σ_8 amplitudes of the models using the DMR data and linear perturbation theory (which is valid on the large scales probed by COBE). As noted in §1, for CDM, COBE yields $\sigma_8 \gtrsim 1$, which implies $\sigma_{\|}$ in excess of 1200 km s^{-1} over scales of a few Mpc. For the other models, COBE's *rms* fluctuations on 10°, including the DMR errors and cosmic variance for the models, imply $\sigma_8 \simeq 0.78 \pm 0.16$ (for C+H13), 0.69 ± 0.14 (for C+H30), 0.53 ± 0.11 (for TILT7), 0.95 ± 0.19 (for ALPHA3), and 0.51 ± 0.10 (for ALPHA5). When normalized to COBE, it is possible to find models with reduced $\sigma_{\|}$. One should, however, point out that models with $\sigma_{\|} \sim 400 - 550\,\mathrm{km\,s^{-1}}$, although favorable over $\sigma_8 = 1$ CDM, may still be inadequate— simulation-to-simulation variations in $\sigma_{\|}$ are typically $\lesssim 100\,\mathrm{km\,s^{-1}}$ (G92), the observed errors in $\sigma_{\|}$ are $\sim 50\,\mathrm{km\,s^{-1}}$, and Bean et al. (1992) found $\sigma_{\|}$ of order $250 \pm 50\,\mathrm{km\,s^{-1}}$.

In fig. 3a we plot $\sigma_{\|}$ for 'favorable' models, subject to the above COBE normalizations. They are: $\sigma_8 = 0.6$ ALPHA5 and $\sigma_8 = 0.5$ TILT7, both consistent with COBE; $\sigma_8 = 0.5$ C+H30, which is somewhat beyond the 1σ level; and $\sigma_8 = 0.5$ CDM, which is inconsistent with COBE and shown here for comparison. We exclude C+H13 and ALPHA3 from our list, as they produce excessive $\sigma_{\|}$. TILT7 and C+H30 both produce small-scale $\sigma_{\|}$ in the $400 - 550\,\mathrm{km\,s^{-1}}$ range, but are still at least 30% above the observed $\sigma_{\|}$. (C+H30 is subject to the uncertainty of our one-fluid model.) The only model in fig. 3a that matches COBE and small-scale $\sigma_{\|}$ is ALPHA5, but it suffers from inadequate halo formation.

4.2 HALO FORMATION

Reducing small-scale power can also help alleviate some problems associated with an excessive number density of high-mass objects that plague the CDM model (White et al. 1987; G92). In order to study halo formation, we simulate models in 51.2 Mpc boxes, again using 128^3 particles and a 256^3 particle-mesh grid. Although adequate for analyzing the halo distribution (G92), the 51.2 Mpc box simulations *cannot* be used to compute $\sigma_{\|}$. (The exact details of galaxy formation require simulations with separate hot and cold dark matter particles and separate dark matter and baryonic matter particles in alpha models. The coupling to the vector field only occurs for the dark matter and can lead to a natural bias between dark and baryonic matter (Gradwohl & Frieman 1992).)

Halos in our simulations are identified as local density maxima in the evolved, nonlinear density field (Bertschinger & Gelb 1991) and are characterized by their circular velocities computed from the enclosed mass within R =300 kpc of the density peak. The distribution within $25\,\mathrm{km\,s^{-1}}$ bins is shown in fig. 3b for the same scenarios as in fig. 3a. The solid line is the observed estimate, using a Schechter (1976) luminosity function and Tully-Fisher (1977) and Faber-Jackson (1976) relationships to relate luminosity to mass, assuming that 70% of the halos are spirals and 30% are ellipticals (G92).

The cases $\sigma_8 = 0.5$ CDM and $\sigma_8 = 0.5$ TILT7 appear to match the observed distribution fairly well. G92 demonstrated, however, that high-mass halos should be divided into clusters of halos so that 1) the simulations contain clusters and 2) extra weight is given to dense systems thereby enhancing the two-point correlation function in biased ($\sigma_8 < 1$) models (White et al. 1987). Therefore, TILT7 actually does much better than CDM—it produces less high-mass halos which, when split up, make up the mid-mass deficit. C+H30 produces too few halos, which can be remedied by evolving the simulation further at the expense of raising $\sigma_{\|}$. ALPHA5 drastically fails to match the observed distribution for $\sigma_8 = 0.6$. (ALPHA3 does better, but it produces excessive $\sigma_{\|}$.)

5. CONCLUSIONS

For $\sigma_8 \gtrsim 0.5$ (the precise value depends on the model), the nonlinear coupling of waves in models with more large-scale and less small-scale power than CDM actually *increases* $\sigma_{\|}$ on small scales, in complete disagreement with linear perturbation theory. At $\sigma_8 = 0.5$, C+H30 and TILT7 (both consistent with COBE) yield $\sigma_{\|} \sim 400-550\,\mathrm{km\,s^{-1}}$ on small scales and they also generate less halos than CDM. The only model which produces $\sigma_{\|} \sim 300\,\mathrm{km\,s^{-1}}$, and at the same time matches COBE, is ALPHA5 at $\sigma_8 = 0.6$, but it fails to produce a sufficient number density of halos. These results are summarized in Table 1.

The fact that it seems difficult to accommodate a low $\sigma_{\|}$, and still have enough small-scale power for adequate halo formation, may hint to a basic problem of $\Omega = 1$ cosmogonies. One way out of this apparent impasse is to lower the matter density of the universe (possibly with a cosmological constant), and thereby maintain a low $\sigma_{\|}$ with increased small scale power. It is clearly too early to view this problem as a death stroke

to $\Omega = 1$ scenarios.

We thank Ed Bertschinger, Dick Bond, Adrian Melott, Bob Schaefer, and Mike Turner for stimulating discussions. This research was conducted using the Cornell National Supercomputer Facility at the Center for Theory and Simulation at Cornell University (funded by the NSF, IBM, and New York State and members of its Corporate Research Institute). This work was supported in part by the DOE and NASA grant NAGW-2381 at Fermilab. B.G. also acknowledges DOE grant #DE-FG03-91ER (40662 Task C) at UCLA.

REFERENCES:

Adams, F. C., Bond, J. R., Freese, K., Frieman, J. A., & Olinto A. V. 1992, preprint

Bean, A. J., Efstathiou, G., Ellis, R. S., Peterson, B. A., & Shanks, T. 1983, MNRAS, 205, 605

Bertschinger, E., Dekel, A., Faber, S. M., Dressler, A., & Burstein, D. 1990, ApJ, 364, 370

Bertschinger, E. & Gelb, J. M. 1991, Computers in Physics, 5, 164

Cen, R., Gnedin, N. Y., Kofman, L. A., & Ostriker, J. P. 1992, preprint

Couchman, H. M. P. & Carlberg, R. 1992, ApJ, 389, 453

Davis, M., Efstathiou, G., Frenk, C. S., & White, S. D. M. 1985, ApJ, 292, 371 (DEFW)

Davis, M. & Peebles, P. J. E. 1983, ApJ, 267, 465

Davis, M., Summers, F. J., & Schlegel, D. 1992, preprint

Faber, S. M. & Jackson, R. E. 1976, ApJ, 204, 668

Frieman, J. A. & Gradwohl, B. 1991, Phys. Rev. Lett., 67, 2926

Gelb, J. M. 1992, M.I.T. Ph.D. thesis (G92);
also Gelb, J. M. & Bertschinger, E. 1992, in preparation;
and Gelb, J. M. 1992, to appear in proc. of Groups of Galaxies Workshop, Space Telescope Science Institute, preprint

Gradwohl, B. & Frieman, J. A. 1992, Ap.J., preprint

Katz, N., Quinn, T., & Gelb, J. M. 1992, preprint

Lightman, A. & Schechter, P. L. 1990, ApJS, 74, 831

Melott, A. L. 1990, Physics Reports, 193, 1

Park, C. 1990, MNRAS, 242, 59

Peebles, P. J. E. 1980, The Large-Scale Structure of the Universe (New Jersey: Princeton University Press)

Schechter, P. L. 1976, ApJ, 203, 297

Smoot, G. F. et al. 1992, preprint

Tully, R. B. & Fisher, J. R. 1977, Astr. Ap., 54, 661

van Dalen, A. & Schaefer, R. K. 1991, preprint

White, S. D. M., Davis, M., Efstathiou, G., & Frenk, C. S. 1987, Nature, 330, 451

TABLE 1
Scorecard

Model	σ_8	COBE	$\sigma_{\|\|}(r \lesssim 3$ Mpc)	Halos
CDM	0.5	−	o	−
C+H30	0.5	+	o	o
ALPHA5	0.6	+	+	−
TILT7	0.5	+	o	+

Table 1 Caption: Scorecard for the various models with + indicating a favorable score, o indicating a marginal score, and − indicating a disfavorable score.

FIGURE CAPTIONS:

Figure 1: a) Linear realizations of power spectra (using the same set of initial random numbers appropriately scaled) normalized to $\sigma_8 = 1$. (C+H30 has less small-scale power than C+H13 and ALPHA5 has less small-scale power than ALPHA3.) b) Nonlinear power spectra at $\sigma_8 = 1$ for some of the simulations shown in fig. 1a. In both a) and b), the solid curve is the analytic form of the DEFW linear CDM power spectrum for discrete $kL/(2\pi)$. The sharp cutoff corresponds to the three-dimensional Nyquist wavenumber. The first bin for the simulated models is an average over 18 waves.

Figure 2: a) Linear theory calculations of $\sigma_{\parallel}$ versus comoving separation (eqn. 3) for $\sigma_8 = 1$. (C+H30 is lower than C+H13 and ALPHA5 is lower than ALPHA3.) b) Nonlinear calculations of $\sigma_{\parallel}$ for CDM (short dashed curves) and for C+H30 (long dashed curves) at four values of σ_8. c) Nonlinear calculations of $\sigma_{\parallel}$ for CDM (short dashed curves), C+H13 (long dashed curves), ALPHA3 (dot-short dashed curves), and TILT7 (dot-long dashed curves) at $\sigma_{\parallel} = 0.5$ and 1. The observed estimates from galaxies for $r \sim 1 - 3$ Mpc are $300 \pm 50\,\mathrm{km\,s^{-1}}$ (Davis & Peebles 1983) and $250 \pm 50\,\mathrm{km\,s^{-1}}$ (Bean et al. 1983).

Figure 3: a) Nonlinear calculations (200 Mpc box) of $\sigma_{\parallel}$. b) Distribution of halos versus circular velocity (in $\Delta V_{\mathrm{circ}} = 25\,\mathrm{km\,s^{-1}}$ bins). The solid curve is the observed estimate. In both a) and b) the cases are: CDM at $\sigma_8 = 0.5$ (short dashed curves), C+H30 at $\sigma_8 = 0.5$ (long dashed curves), ALPHA5 at $\sigma_8 = 0.6$ (dot-short dashed curves), and TILT7 at $\sigma_8 = 0.5$ (dot-long dashed curves).

FIG. 1

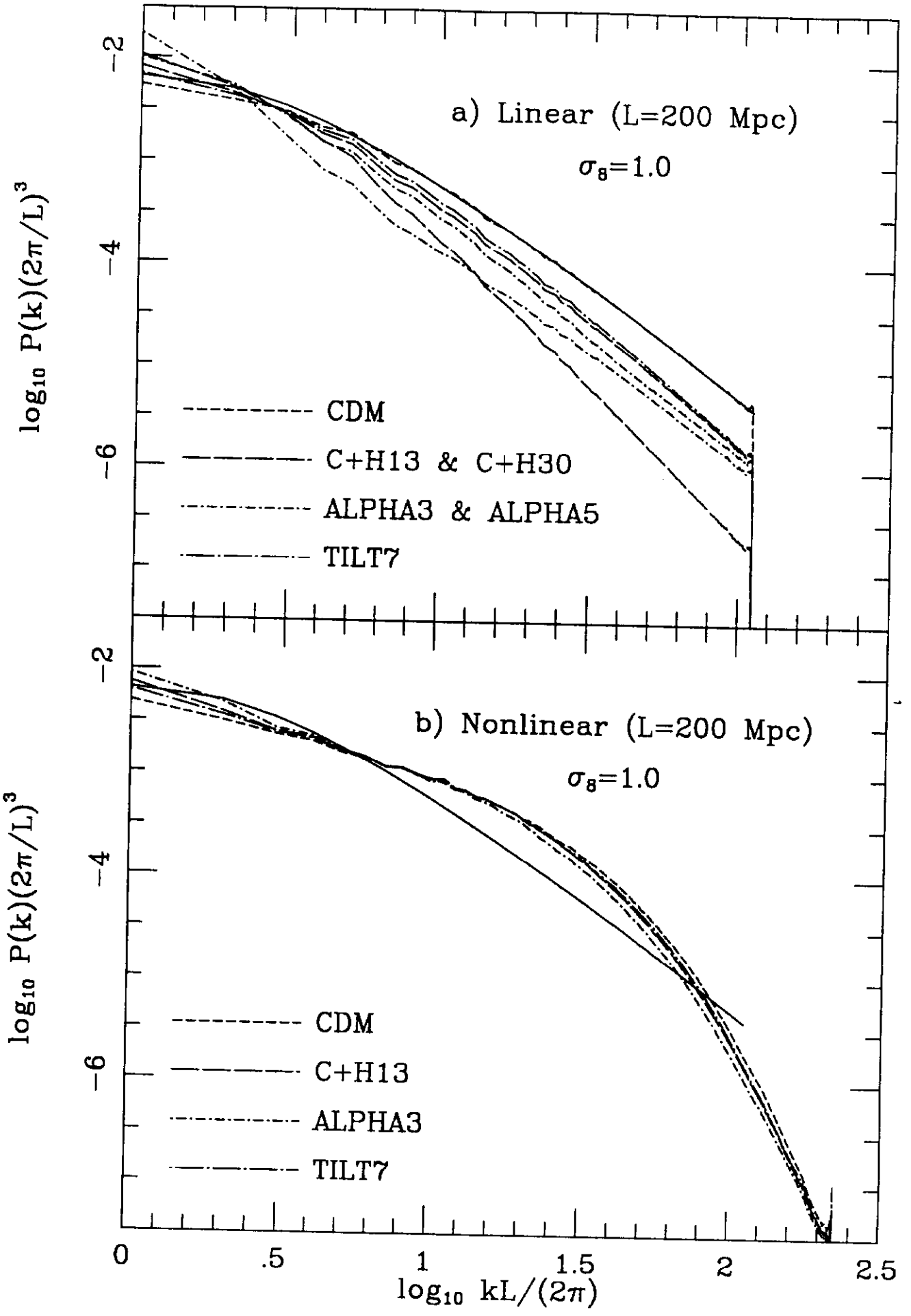
a) Linear (L=200 Mpc)
σ_8=1.0
CDM
C+H13 & C+H30
ALPHA3 & ALPHA5
TILT7
b) Nonlinear (L=200 Mpc)
σ_8=1.0
CDM
C+H13
ALPHA3
TILT7
$\log_{10} P(k)(2\pi/L)^3$
$\log_{10} kL/(2\pi)$
-2
-4
-6
0
.5
1
1.5
2
2.5

FIG. 2

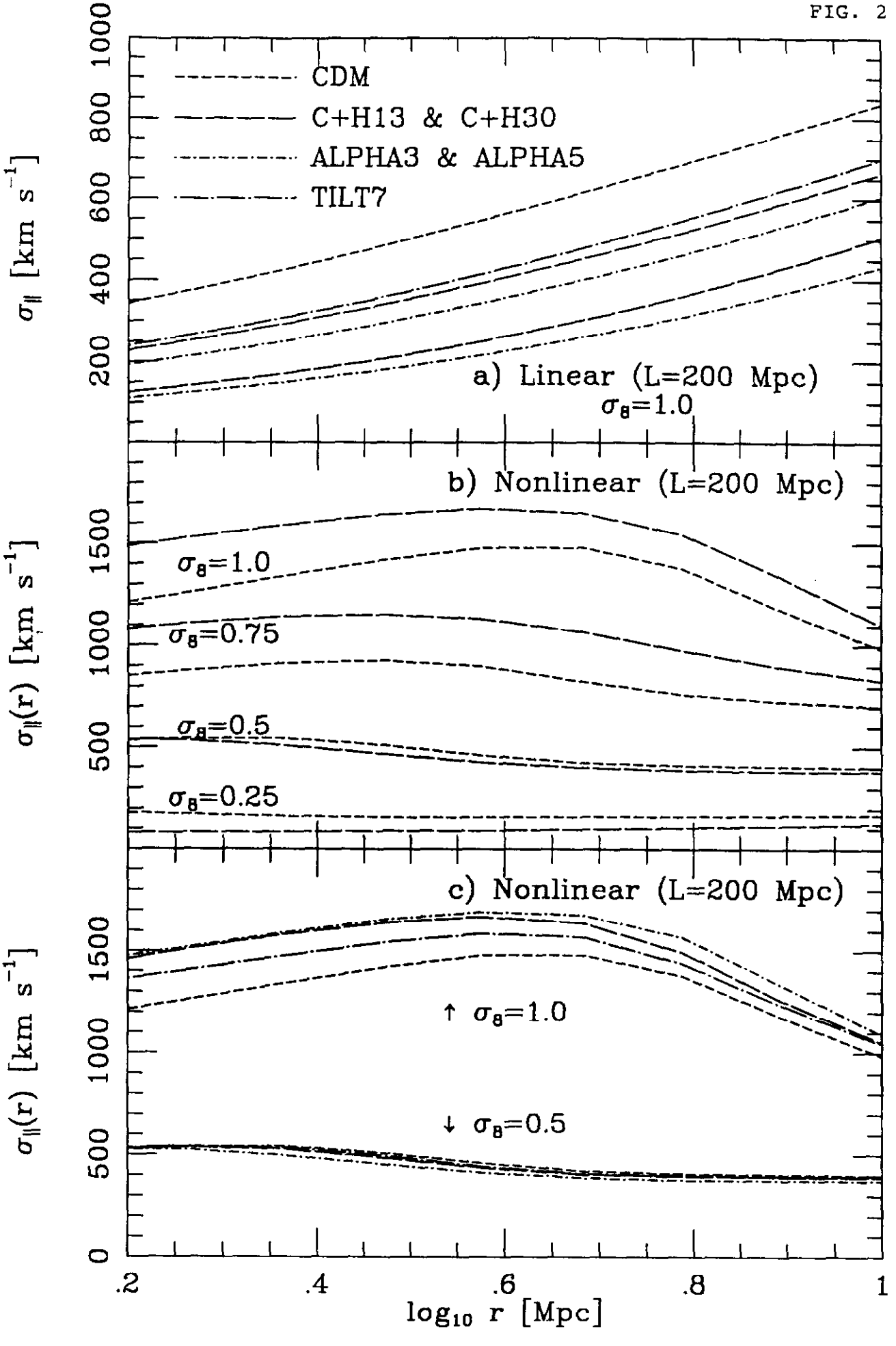
CDM
C+H13 & C+H30
ALPHA3 & ALPHA5
TILT7
a) Linear (L=200 Mpc)
σ8=1.0
b) Nonlinear (L=200 Mpc)
σ8=1.0
σ8=0.75
σ8=0.5
σ8=0.25
c) Nonlinear (L=200 Mpc)
↑ σ8=1.0
↓ σ8=0.5
σ∥ [km s⁻¹]
σ∥(r) [km s⁻¹]
σ∥(r) [km s⁻¹]
log10 r [Mpc]
0
200
400
500
600
800
1000
1500
.2
.4
.6
.8
1

FIG. 3

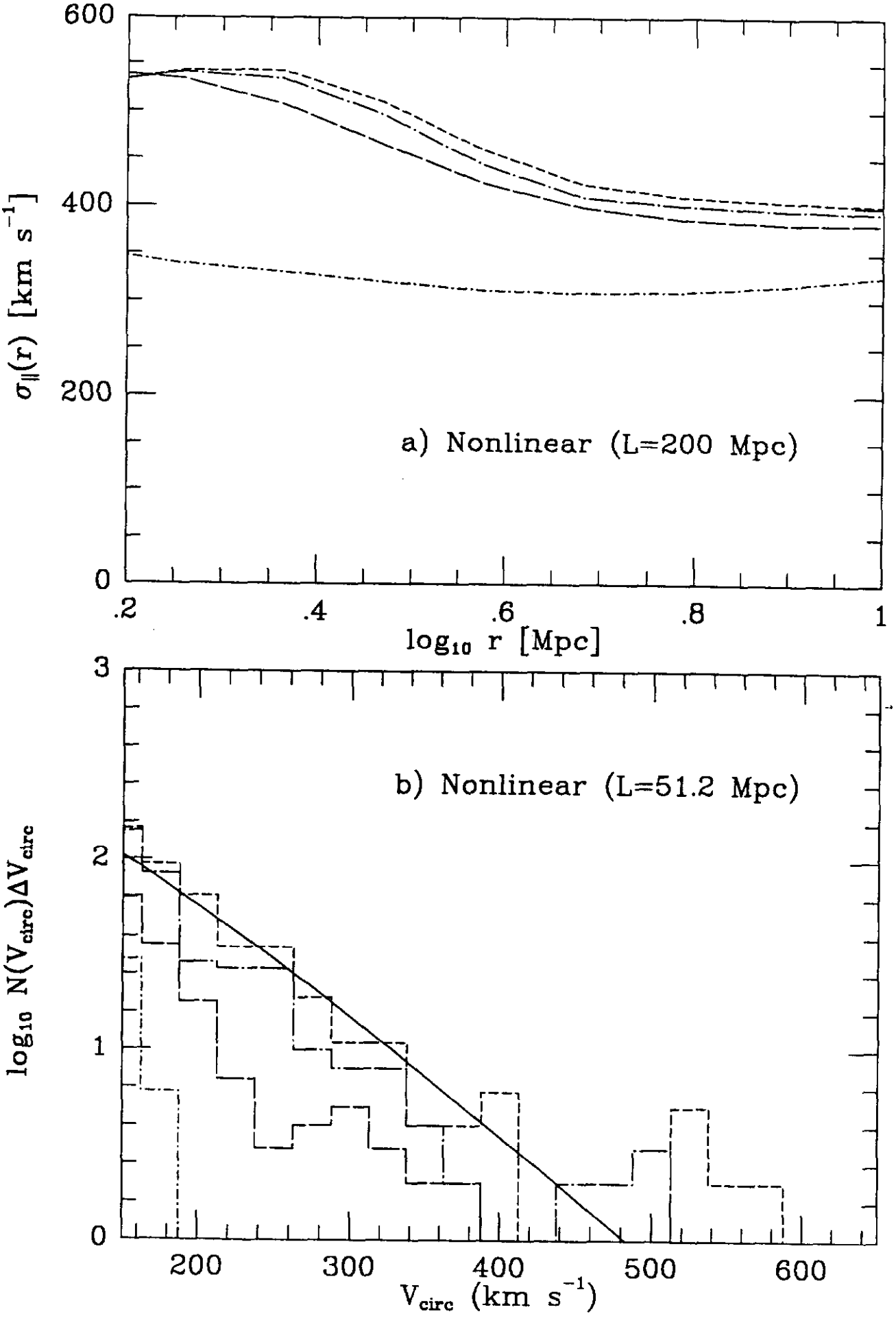
600
400
200
0
$\sigma_{\parallel}(r)$ [km s^{-1}]
a) Nonlinear (L=200 Mpc)
.2
.4
.6
.8
1
$\log_{10}$ r [Mpc]
3
2
1
0
$\log_{10}$ N(V_{circ})ΔV_{circ}
b) Nonlinear (L=51.2 Mpc)
200
300
400
500
600
V_{circ} (km s^{-1})